



Compact and tunable stretch bioreactor advancing tissue engineering implementation. Application to engineered cardiac constructs

Giovanni Putame^{a,b}, Stefano Gabetti^{a,b}, Dario Carbonaro^{a,b}, Franca Di Meglio^c,
Veronica Romano^c, Anna Maria Sacco^c, Immacolata Belviso^c, Gianpaolo Serino^{a,b},
Cristina Bignardi^{a,b}, Umberto Morbiducci^{a,b}, Clotilde Castaldo^c, Diana Massai^{a,b,*}

^a PolitoBIOMed Lab, Department of Mechanical and Aerospace Engineering, Politecnico di Torino, Turin, Italy

^b Interuniversity Center for the Promotion of the 3Rs Principles in Teaching and Research, Italy

^c Department of Public Health, University of Naples "Federico II", Naples, Italy

ARTICLE INFO

Article history:

Received 15 March 2020

Revised 14 July 2020

Accepted 22 July 2020

Keywords:

Bioreactor

Cyclic stretching

Mechanical stimulation

Tissues engineering

Cardiac tissue maturation

ABSTRACT

Physical stimuli are crucial for the structural and functional maturation of tissues both *in vivo* and *in vitro*. In tissue engineering applications, bioreactors have become fundamental and effective tools for providing biomimetic culture conditions that recapitulate the native physical stimuli. In addition, bioreactors play a key role in assuring strict control, automation, and standardization in the production process of cell-based products for future clinical application. In this study, a compact, easy-to-use, tunable stretch bioreactor is proposed. Based on customizable and low-cost technological solutions, the bioreactor was designed for providing tunable mechanical stretch for biomimetic dynamic culture of different engineered tissues. In-house validation tests demonstrated the accuracy and repeatability of the imposed mechanical stimulation. Proof of concepts biological tests performed on engineered cardiac constructs, based on decellularized human skin scaffolds seeded with human cardiac progenitor cells, confirmed the bioreactor Good Laboratory Practice compliance and ease of use, and the effectiveness of the delivered cyclic stretch stimulation on the cardiac construct maturation.

© 2020 IPEM. Published by Elsevier Ltd. All rights reserved.

1. Introduction

Tissue engineering (TE) is a multidisciplinary research field whose primary purpose is the *in vitro* development of functional tissue constructs used as models for basic research, drug testing, and disease investigations, or ultimately aimed at repairing injured tissues or even organs [1,2]. According to the TE paradigm, the bio-process for generating functional constructs is based on three key elements: cells, scaffolds, and culture environmental cues [3,4].

Cells play a crucial role, since they generate the new tissue through proliferation, differentiation and maturation. In particular, the use of human stem or progenitor cells, which can differentiate into tissue-specific functional cell types, provides promising perspectives for patient-specific tissue models and personalized TE [5–10].

Scaffolds substantially serve as active biochemical and structural support for cell growth. In particular, decellularized extra-

cellular matrix (ECM) is recognized as one of the most promising biological scaffolds, because of its native biochemical and biomechanical features, and its three-dimensional (3D) microarchitecture [11,12].

Lastly, biomimetic chemical and physical environmental cues have proven to be fundamental for defining the fate and the functionality of the engineered constructs [13–16]. Focusing on strategies for engineering tissues that *in vivo* are physiologically subjected to mechanical stimuli (e.g., tensile or compressive load), several studies demonstrated that the use of dynamic culture devices providing adequate *in vitro* mechanical stimuli leads to significant improvements in structural and functional tissue maturation [17–20]. For example, it was observed that the controlled exposure of engineered skeletal muscle tissues to mechanical cyclic stretch promotes their development, with improved morphological, contractile and myogenic properties [21–24]. Furthermore, stretch was successfully applied for cultivating *in vitro* tendon and ligament grafts, with several studies demonstrating that mechanical stimulation is crucial for promoting tenocyte differentiation, tendon matrix synthesis, and construct tensile strength [25–30]. Dynamic culture devices providing stretch stimuli were also used for generat-

* Corresponding author at: PolitoBIOMed Lab, Department of Mechanical and Aerospace Engineering, Politecnico di Torino, Turin, Italy.
E-mail address: diana.massai@polito.it (D. Massai).

ing skin tissue models characterized by thick epidermal layers with high levels of expressed basement membrane proteins [31], and for *ex vivo* expansion of skin grafts, promoting dermal ECM synthesis [32,33]. Cyclic stretch plays a fundamental role in bioprocesses designed for the *in vitro* maturation of cardiac tissue models. A large body of literature demonstrated that the provision of cyclic stretch stimulation mimicking the cyclic diastolic filling of the ventricles promotes cell proliferation, myocardium-like morphological arrangement and maturation, and contractile performance of engineered cardiac tissues [34–42].

The need of TE bioprocesses to provide biomimetic physical stimuli in a strictly controlled manner is faced using bioreactors. When equipped with advanced and programmable technological solutions, these devices can guarantee control, automation, and standardization of the production process [43,44], fulfilling the rigorous requirements for clinical translation of cell-based products. Moreover, bioreactors represent useful platforms for generating *in vitro* tissue models, thus addressing the need for providing investigation methods alternative to animal-based experimentation.

However, bioreactor-based approaches have to cope with a series of drawbacks limiting their wide spread. In particular, complex technology and high costs, often related to the high level of customization required by the specific application, represent relevant limiting factors [45]. Moreover, difficulty of use is a critical aspect affecting both custom-made and commercial bioreactor platform diffusion [46,47].

Nowadays, the availability of affordable open-source and low-cost electronic solutions for bioprocess monitoring and control purposes and the diffusion of low-cost 3D printing technologies give the opportunity to rethink the design phase as well as to develop highly customizable and flexible bioprocess platforms at limited implementation costs [48–52]. In this perspective, we present here a compact, easy-to-use, tunable stretch bioreactor platform for TE applications. Customizable and low-cost technological solutions are adopted for the platform implementation. Using a purpose-built test bench, in-house validation tests are performed to assess the motor motion accuracy and repeatability. To demonstrate the bioreactor platform performance in a cell culture laboratory and to investigate the impact of cyclic stretch on maturation of engineered cardiac tissues, explanatory biological experiments on decellularized human skin (d-HuSk) scaffolds seeded with human cardiac progenitor cells (hCPCs), performed within the bioreactor platform, are presented. The hCPC-seeded d-HuSk scaffolds are subjected to controlled cyclic stretch, and the effect of cyclic stretch conditioning is analyzed in terms of cell organization and gene expression of typical cardiac markers.

2. Materials and methods

2.1. Bioreactor platform

The design of the bioreactor platform was guided by specific requirements. Firstly, the device should provide tunable mechanical stretch for biomimetic dynamic culture of different engineered tissues (e.g., myocardium, skeletal muscle, skin, tendon, and ligament tissue). Then, it should accomplish general specifications of a bioreactor for TE strategies [17], particularly Good Laboratory Practices (GLP) compliance in terms of ease of assembling, cleaning, and use in a cell culture laboratory and with conventional laboratory equipment. Moreover, the bioreactor platform should be modular for facilitating assembling/disassembling/cleaning procedures and customization, and it should be characterized by small size, to be easily handled under laminar flow hood and within the incubator. Lastly, for promoting the use of the system, the bioreactor platform should be designed and produced with easy-to-use and low-cost hardware and software, and overall it should guarantee

Table 1
Stimulation parameter combinations. Black dots indicate the available combinations.

		Frequency (Hz)		
		1	2	3
Amplitude range (mm)	2.1–3	•		
	1.1–2	•	•	
	0.1–1	•	•	•

reliability for long-term experiments within the incubator (37 °C, 5% CO₂, and 90–95% humidity).

Based on these requirements, the bioreactor platform is designed consisting of three main units (Fig. 1A): (1) the culture unit, housing the constructs; (2) the stimulation unit, providing the biomimetic mechanical stimuli; (3) the control unit, devoted to the control of the stimulation unit. Both the culture unit and the stimulation unit are mounted on an aluminum planar base (342 mm x 128 mm) to be incubated, while the control unit is located outside the incubator.

In detail, the culture unit, adapted from a previously developed device [53], is composed of a polycarbonate culture chamber (140 × 80 × 75 mm³ with a priming volume of ~100 ml) designed to house multiple constructs to be cultured simultaneously. Within the culture chamber, two opposite polyoxymethylene (POM) clamps allow grasping the constructs during stimulation. One clamp is mobile, coupled with a stainless steel through-shaft externally connected to the stimulation unit motor, while the opposite clamp is fixed (Fig. 1B). Silicone bellows (J-Flex rubber, Retford, UK) assure watertightness of the culture chamber. The culture chamber is inserted within an L-shaped chassis, previously developed for guaranteeing a correct positioning of the culture chamber on the planar base [54]. The stimulation unit consists of a watertight box (130 × 95 × 65 mm³), which houses a captive stepper motor (NEMA 14, Nanotec Electronic GmbH & Co. KG, Feldkirchen, DE) that generates a linear motion with a resolution of 10 μm/step. The motor provides the mechanical stimulation to the cultured constructs, controlled by the control unit. The latter is made of a compact box (170 × 150 × 60 mm³) containing a microcontroller board (Arduino Due, Arduino, Ivrea, IT), selected because it is an open-source and low-cost electronics platform, which is coupled with a small-sized motor driver (A4988, Allegro MicroSystems, Manchester, USA). The motor driver with built-in translator and current regulator acts as bridge component between the microcontroller and the motor, and enables motor control in open-loop configuration efficiently assuring the needed power supply. A user-friendly interface, based on push buttons and a 1.8" LCD screen (Arduino), allows the proper adjustment of the initial relative position between clamps and the setting of the stimulation parameters (i.e., stretching amplitude and frequency). A schematic diagram of the control unit implementation is reported in Figure 1C.

To perform the explanatory biological tests, dedicated to culture cardiac constructs under cardiac-like cyclic stretch, the microcontroller is programmed to generate a sinusoidal motor motion with tunable stretching amplitudes (0.1–3.0 mm, by 0.1 mm steps) and frequencies (1–3 Hz, by 1 Hz steps). Available combinations of stimulation parameters for culturing constructs are reported in Table 1.

All culture chamber components in contact with medium or constructs are made of cytocompatible and autoclavable materials [53,55]. The L-shaped chassis housing the culture chamber and the stimulation unit box are manufactured in ABS thermoplastic material by fused deposition modelling (FDM) for guaranteeing design flexibility and cost-efficiency [54].

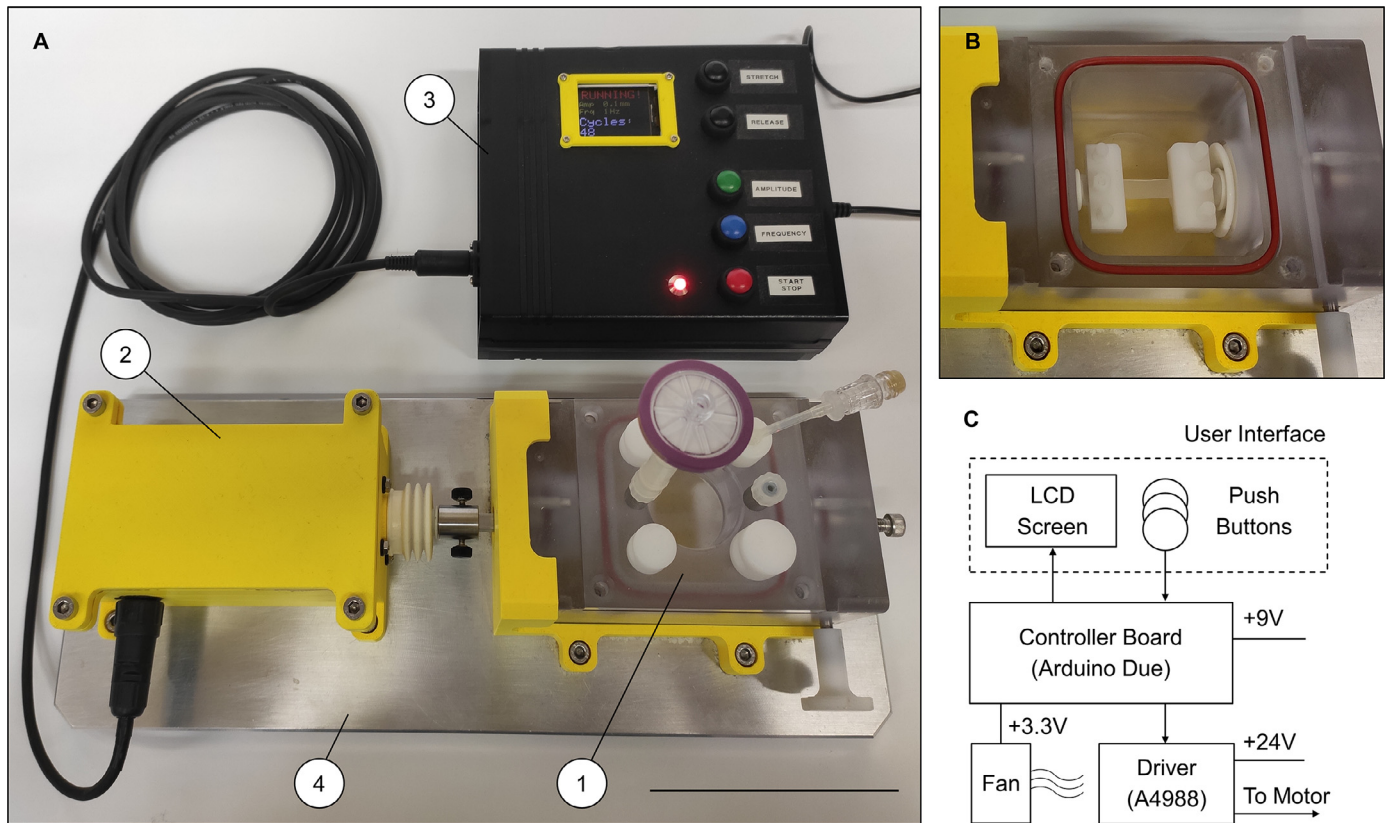


Figure 1. Bioreactor platform. (A) Top view of the bioreactor platform: 1) Culture unit; 2) Stimulation unit; 3) Control unit; 4) Planar base. Scale bar = 100 mm. (B) Top view of the open culture chamber with the clamps and an explanatory silicone patch. (C) Schematic diagram of the control unit implementation.

2.2. In-house tests

The ease of use and the reliability of stimulation and control units were preliminarily tested in-house. In detail, the motion accuracy of the stimulation unit operated by the control unit was characterized using a purpose-built test bench. A linear variable displacement transducer (LVDT, AML/EU/±5/S, Applied Measurements Ltd., Aldermaston, UK), mounted on a chassis and connected to a dedicated data acquisition system (Personal computer equipped with a cDAQ-9174 coupled with a NI 9218 module, National Instruments, Austin, TX, USA), was put in contact with the through-shaft connected to the stimulation unit motor (Supplementary Fig. S1), and all the 60 combinations of motor amplitude and frequency parameters were tested. In detail, for each possible combination, the motor imparted displacement was acquired continuously over 30 cycles (sampling rate = 1652 Hz). The measured LVDT signals were acquired, filtered (Butterworth low-pass filter, order 8, cut-off frequency = 10 Hz), and analyzed in LabVIEW environment (LabVIEW, National Instruments) to evaluate the peak-to-peak amplitude as well as the frequency of the recorded displacement signals. All measurements were carried out in triplicate. The motor displacement waveforms were characterized by comparing the measured waveforms with the prescribed ideal sinusoidal waveforms. The mean percentage errors of measured amplitude and frequency values with respect to the prescribed nominal values were expressed as mean ± standard deviation (SD).

2.3. Biological tests

2.3.1. Bioreactor platform performance in a cell culture laboratory

The bioreactor platform was then tested in a cell culture laboratory in order to assess its ease of use and compliance with

GLP procedures. In detail, the components of the culture chamber were autoclaved and assembled under laminar flow hood, the culture chamber was filled with Dulbecco's Modified Eagle's Medium/Ham's Nutrient Mixture F12 culture medium (Sigma-Aldrich, St. Louis, MO, USA), and the assembled system was placed in incubator without constructs but with the mechanical stimulation (1 mm, 1 Hz) switched on for 5 days.

2.3.2. Preparation and culture of cardiac constructs

To investigate the influence of biomimetic cyclic stretch on the maturation of cardiac constructs, explanatory biological tests were carried out on decellularized human skin (d-HuSk) scaffolds seeded with human cardiac progenitor cells (hCPCs) and hCPC-derived early cardiac myocytes.

Concerning the scaffold preparation, human skin samples were obtained from patients undergoing abdominoplasty ($n = 4$, mean age 41.75 ± 2.36). Upon receipt, samples were washed in physiological saline solution, then subcutaneous tissue was removed and multiple specimens were cut (length = 20 mm, width = 10 mm) marking Langer's line orientation. For decellularization treatment, specimens were enclosed in embedding cassettes housed in a purpose-built sample-holder, put within a beaker filled with the decellularizing solution (700 ml) and placed on a magnetic stirrer, and kept under constant stirring (150 rpm) for 24 h [56]. The decellularizing solution contained 1% w/v sodium dodecyl sulfate (SDS) (Sigma-Aldrich) and 1% v/v Triton (Sigma-Aldrich). The specimens were then rinsed for 24 h in antibiotic solution containing 0.25 µg/ml Amphotericin B, 100 U/ml Penicillin, and 50 U/ml Streptomycin (all from Sigma-Aldrich) in PBS, and lastly in sterile bidistilled water for additional 30 min [57,58]. The d-HuSk specimens were snap-frozen, mounted on a cryostat chuck using Tissue Freezing Medium (Leica Microsystems, Wetzlar, Germany), and

sliced into 600- μm -thick sections by a Leica CM1950 cryostat (Leica Microsystems). Cryosections of d-HuSk were sterilized by exposure to ultraviolet radiation for 40 min and rehydrated for one week with F12K medium in incubator (37 °C, 5% CO₂). The sterilized and rehydrated d-HuSk cryosections were then stored in standard culture conditions with the same medium until use.

As regards the hCPCs, they were isolated from cardiac specimens derived from macroscopically uninjured areas of the left ventricle of explanted hearts of patients undergoing heart transplant because of end-stage heart failure ($n = 10$, mean age 49.5 ± 4.7). Specifically, following a previously described protocol [59] cardiac specimens were washed in physiological saline solution, dissected, minced, and enzymatically disaggregated by incubation in 0.25% trypsin (Sigma-Aldrich) for 6 h at 4 °C and in 0.1% w/v collagenase II (Sigma-Aldrich) for 30 min at 37 °C. The digestion was stopped by adding double volume of Hanks' Balanced Salt solution (Sigma-Aldrich) supplemented with 10% fetal bovine serum (FBS) (Sigma-Aldrich). Resulting fragments of tissue were further disaggregated by pipetting. Tissue debris and cardiomyocytes were then removed by sequential centrifugation at 100 g for 2 min, passage through a 40- μm cell strainer (BD Biosciences, Franklin Lakes, NJ, USA), and centrifugation at 400 g for 5 min. The obtained cell population was then incubated with anti-fibroblast MicroBeads (Miltenyi Biotec, Bergisch Gladbach, Germany) to magnetically label fibroblasts that were then removed loading cells onto a MACS column (Miltenyi Biotec) placed in the magnetic field of a MACS separator (Miltenyi Biotec). The negative fraction of unlabeled hCPCs ran through the column was collected and plated at a density of 4×10^3 cells per cm² in F12K medium, prepared from Nutrient Mixture F-12 Ham medium (Sigma-Aldrich) supplemented with 10% FBS (Sigma-Aldrich), basic fibroblast growth factor (PeproTech, Rocky Hill, NJ, USA), glutathione (Sigma-Aldrich), penicillin and streptomycin (Sigma-Aldrich). The hCPCs were cultured in incubator (37 °C, 5% CO₂) and observed daily by an inverted phase-contrast microscope (Olympus, Tokyo, Japan). Medium was replaced every 3 days until the 75% confluence was reached. Then, an unselected subpopulation of hCPCs was induced to differentiate towards cardiac myocytes by adding 50 $\mu\text{g}/\text{ml}$ of ascorbic acid (Sigma-Aldrich) and 10 ng/ml of Vascular-Endothelial Growth Factor (Sigma-Aldrich) to the culture medium for 24 days.

Successively, the d-HuSk scaffolds ($n = 7$) were seeded with 2.5×10^6 hCPCs and 2.5×10^6 hCPC-derived early cardiac myocytes. After 7 days of static culture in Petri dish, half of the constructs ($n = 12$) were transferred, in pairs, into the bioreactor culture chamber with F12K medium and subjected to dynamic conditions (i.e., sinusoidal cyclic stretch, 10% strain, 1 Hz) for additional 7 days (see Supplementary Movie 1) for mimicking the cyclic diastolic filling of the ventricles [60–63]. As control experiment, the other half of the constructs ($n = 12$) were cultured statically in Petri dishes for the entire duration of 14 days (Fig. 2). Finally, constructs were cut into smaller specimens that were either fixed in 10% neutral-buffered formalin (Sigma-Aldrich) for morphological analyses or processed for RNA extraction for gene expression profiling.

2.3.3. Histochemistry analysis

Following standard protocols, subsets of constructs cultured in static conditions (control) or in bioreactor and fixed in 10% neutral-buffered formalin were dehydrated in a graded series of alcohols, embedded in paraffin and sliced into serial 5- μm -thick sections [57,58]. Sections were stained with Hematoxylin and Eosin (H&E) and with Mallory's trichrome staining using specific kits (both from Bio-Optica, Milan, Italy). Stained sections were observed by at least three independent researchers using a light microscope DM2000 Led (Leica Microsystems) equipped with an ICC50HD camera (Leica Microsystems).

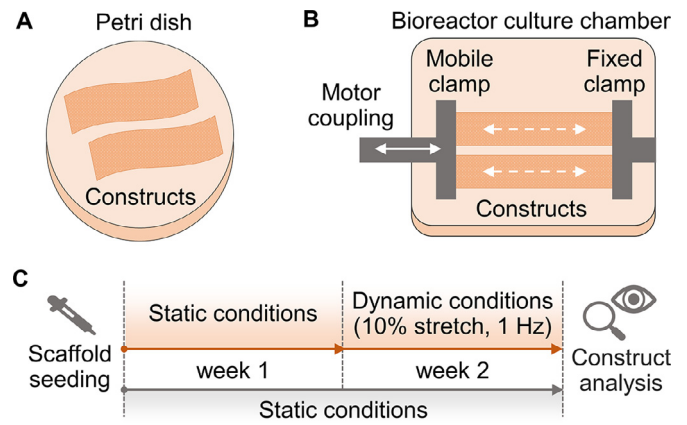


Figure 2. Static versus dynamic culture experimental plan. (A) Constructs in static conditions. (B) Constructs in dynamic conditions, grasped between the two opposite clamps. (C) Timeline of the performed culture protocols.

2.3.4. Gene expression profile analysis

Total RNA was extracted from hCPCs seeded on d-HuSk scaffolds, cultured both in static and cyclic stretch conditions, using Trizol Reagent (Invitrogen, Thermo Fisher Scientific, Carlsbad, CA, USA), according to the manufacturer's instructions. RNA was dissolved in RNase-free water and its final concentration was quantified at the NanoDrop 1000 spectrophotometer (Thermo Scientific, Waltham, MA, USA). All RNA samples were checked for quality and resulted suitable for gene expression profiling analyses. Analysis was performed as previously described [64]. Briefly, RNA from each sample was reverse transcribed into cDNA with QuantiTect Reverse Transcription Kit (Qiagen, Hilden, Germany) and gene expression was quantified by real-time qPCR using Power SYBR Green PCR Master Mix (Applied Biosystem, Thermo Fisher Scientific). DNA amplification was carried out using QuantStudio™ 5 Real-Time PCR System (Thermo Fisher Scientific) and the detection was performed by measuring the binding of the fluorescent dye SYBR Green I to double-stranded DNA. The thermal cycling conditions included an initial enzyme activation at 95 °C for 10 min and 40 cycles consisting of a denaturation step at 95 °C for 15 s and an annealing step at 60 °C for 60 s. Melt curve analysis was performed to assess uniformity of product formation, primer dimer formation and amplification of non-specific products. Primers used in this study were designed with Primer3 software (<http://frodo.wi.mit.edu>) starting from the CDS (coding sequence) of mature mRNA available on GeneBank (Supplementary Table S1). All samples were tested in triplicate with the housekeeping gene (GAPDH) to correct for variations in RNA quality and quantity. Comparative quantification of target gene expression in the samples was performed based on cycle threshold (Ct) normalized to the housekeeping gene and using the $2^{-\Delta\Delta\text{Ct}}$ method.

2.3.5. Statistical analysis

Data from gene expression profiling were analyzed by GraphPad Prism 5.0 (GraphPad Software, La Jolla, CA, USA) using Student's two-tailed unpaired *t*-test. All experiments were performed in triplicate and data were averaged and expressed as the mean \pm standard error of the mean. The statistical significance is denoted as * for p -value ≤ 0.05 , ** for p -value ≤ 0.01 , *** for p -value ≤ 0.001 .

3. Results

3.1. In-house tests

In-house tests confirmed the ease of use and the reliability of the stimulation and control units. In detail, tests on motor imposed

displacement accuracy highlighted that real displacement waveforms agree with the prescribed ideal sinusoidal waveforms for all the available combinations of working conditions, as testified by the explanatory waveforms presented in Figure 3A. As regards the comparison between the measured stretching amplitude values and the nominal ones, mean error values up to $13.3\% \pm 7.3\%$ were observed, with the largest deviation from the nominal curve corresponding to the combination characterized by minimum amplitude equal to 0.1 mm and frequency equal to 1 Hz. For nominal amplitude values higher than 0.4 mm the observed mean error values were lower than 4% (Fig. 3B). Concerning the nominal frequency, mean error values up to 10.5% (corresponding to the combination characterized by amplitude equal to 1.3 mm and frequency equal to 1 Hz) were observed (Fig. 3C).

3.2. Biological tests

3.2.1. Bioreactor platform performance in a cell culture laboratory

Preliminary tests performed in a cell culture laboratory confirmed ease of use, sterility maintenance, and functionality of the bioreactor platform in a standard incubator. During the explanatory cyclic stimulation tests run for 5 days in incubator, the system did not present adverse issues, the watertightness of the culture chamber and the stimulation unit was confirmed, and the culture medium did not present any signs of contamination.

3.2.2. Histochemistry

The H&E and Mallory's trichrome staining of the cardiac constructs revealed that, under both static (control) and dynamic (sinusoidal cyclic stretch, 10% strain, 1 Hz) culture conditions, hCPCs organized into a structured multilayered tissue on the surface of the d-HuSk scaffolds (Fig. 4). Noteworthy, the histochemical analysis highlighted that the dynamic culture promoted hCPC migration towards the inner layers of the scaffolds (Fig. 4B and D).

3.2.2. Gene expression profile analysis

The gene expression profile analysis of hCPCs extracted from constructs cultured under either static or dynamic conditions included genes typical of main cardiac cell lineages. In particular, in bioreactor-cultured constructs, a significant up-regulation of cardiac alpha actin (ACTC1), a marker typical of late differentiating and mature cardiac myocytes, was observed. On the opposite, markers typical of undifferentiated hCPCs (like CD117) or of early stages of cardiac myocyte differentiation (like TBX3 and TBX5) were significantly down-regulated with respect to control constructs (Fig. 5). The transcription of other markers typical of cardiac myocytes, like MEF2C, CX43, and GATA4, did not differ significantly among constructs cultured in static or dynamic conditions, and similarly happened for the transcription of the mesenchymal cell marker CD105 and of genes typical of smooth muscle cells (GATA6, ACTA2) and endothelial cells (ETS1, FVIII) (Supplementary Fig. S2).

4. Discussion

In TE research, a number of studies demonstrated that successful strategies for the *in vitro* generation of functional engineered tissues require a synergistic combination of appropriate cells, scaffolds, and biochemical and biophysical signals [65–67]. As specifically concerns mechanical cues, in the last two decades a plethora of custom-made bioreactors providing *in vitro* biomimetic mechanical stretch has been proposed [23,24,29–31,33,40,42]. In parallel, ready-to-use systems have been developed by commercial companies (e.g., Tissue Train 3D Culture System from FlexCell International, Hillsborough, USA; TC-3 from Ebers Medical Technology,

Zaragoza, Spain; MCT6 from CellScale, Waterloo, Canada; BioDynamic 5100 from TA Instruments, New Castle, USA). All the developed culture devices substantially contributed to unravel the fundamental role that mechanical stretch has on structural and functional development of biological tissues and in regulating tissue homeostasis and pathophysiology. Moreover, their use increased the knowledge on sensitivity of cells to mechanical stimuli, to which cells react activating specific mechanotransduction pathways that can lead to phenotypic changes [68–71].

However, the proposed custom-made bioreactors were often based on complex technological solutions, difficult to use by non-trained operators in a cell culture laboratory and typically dedicated to highly specialized applications, while the commercial devices are generally expensive and not fully customizable.

Taking into account these limitations, in this study we developed a compact, easy-to-use, tunable stretch bioreactor platform for culturing *in vitro* 3D engineered constructs under biomimetic stretch conditions. Particular attention was paid in developing reliable and affordable stimulation and control units. As regards the stimulation unit, the use of a captive stepper motor enables the provision of linear motion adopting an open loop control strategy ensuring high displacement resolution without the need for additional and complex feedback sensing solutions. In combination, a compact control unit, based on low-cost open-source hardware and freeware software, avoids the use of cumbersome and expensive equipment (e.g., laptop, data acquisition module, and commercial software). Moreover, the integrated user-friendly interface allows ease-of-use to not experienced operators as well as system portability. In-house performance tests confirmed that the bioreactor platform is reliable in providing accurate and repeatable stimulation within a range of physiological interest. For imposed motor displacement values higher than 0.4 mm, the mean error values between the measured amplitude values and the nominal ones were lower than 4%, thus negligible, for all available stimulation parameter combinations. Conversely, for motor displacement values in the range of 0.1 - 0.4 mm, higher amplitude errors were calculated (Fig. 3). However, it should be noted that such small displacement values are not commonly adopted for mechanical stimulation of macroscopic constructs. This inaccuracy could be ascribed to the axial play of the motor shaft, and to inertial and vibrational phenomena that are intrinsic to stepper motors. In addition, possible signal artefacts during the LVDT data acquisition, due to inductive and capacitive electrical interference, could not be excluded. As concerns the stimulation frequency, measurements revealed negligible errors, probably ascribable to intrinsic technical limitations of the adopted low-cost microcontroller.

Preliminary tests in a cell culture laboratory demonstrated that the device is easy-to-use with GLP compliant procedures, compact to handle and fit in a standard incubator, and guarantees watertightness, sterility maintenance and functionality.

For investigating the effect of cyclic stretch on cardiac construct maturation, the biological experiments were performed on decellularized human skin scaffolds seeded with hCPCs and cultured for 7 days in static conditions, and then transferred into the bioreactor (sinusoidal cyclic stretch, 10% strain, 1 Hz) for additional 7 days. The histochemical analysis showed cell engraftment on the scaffold surface in both controls and dynamically cultured constructs (Fig. 4), but only when subjected to cyclic stretch cells migrated towards the inner layers of the scaffolds, starting to colonize their 3D structure (Fig. 4B and D). The gene expression analysis highlighted a significant up-regulation of the ACTC1 marker, typical of late differentiating and mature cardiac myocytes, concomitantly with a marked down-regulation of CD117, TBX3 and TBX5 markers (Fig. 5), typical receptors for stem cells or early stage cardiac myocytes, suggesting that dynamic culture likely promoted hCPC dif-

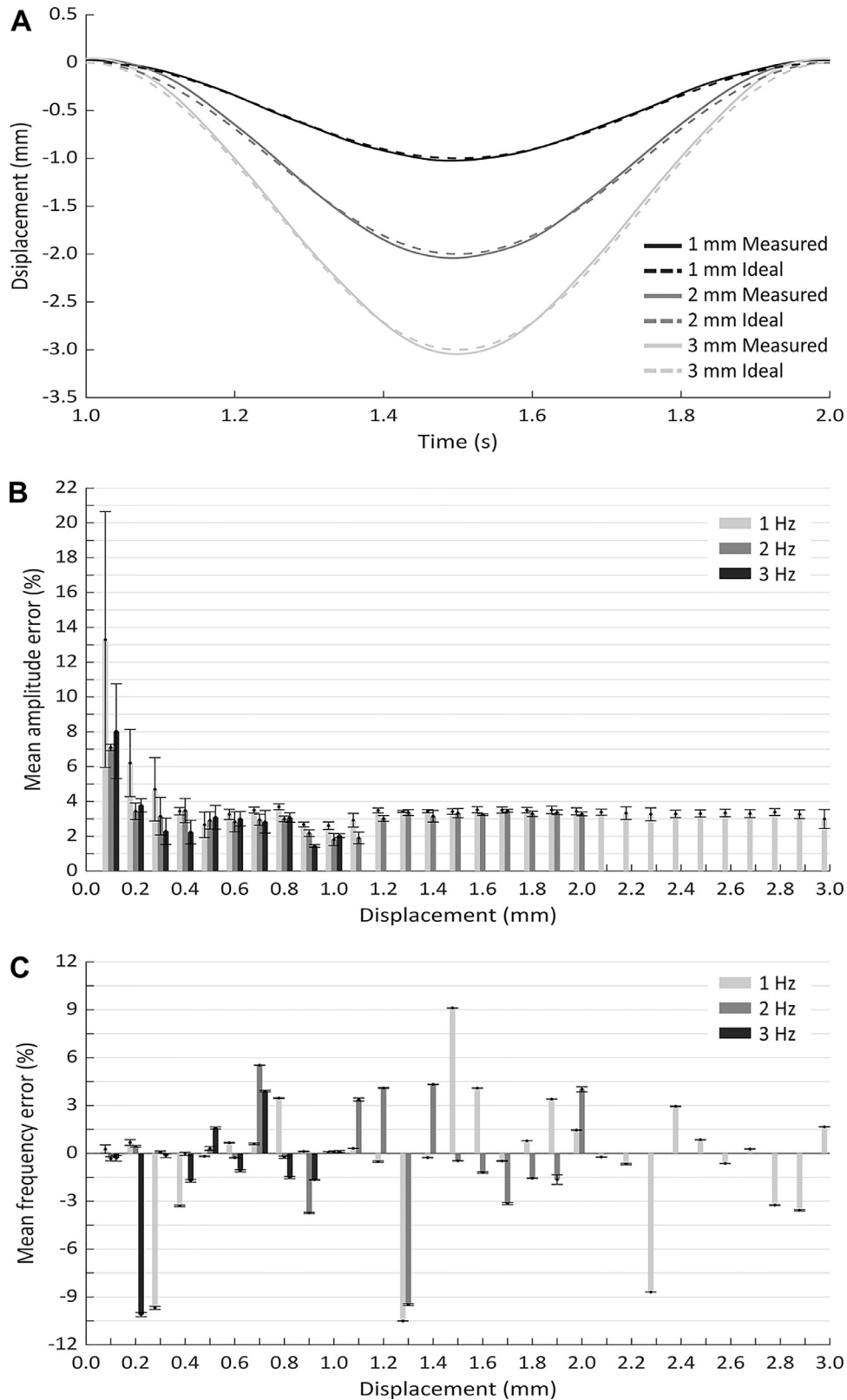


Figure 3. Motor motion performance. (A) Comparisons between measured and ideal sinusoidal motion waveforms for an explanatory stimulation at 1 Hz. (B) Mean percentage errors between measured and nominal stretching amplitude values for all the available combinations. (C) Mean percentage errors between measured and nominal frequency values for all the available combinations.

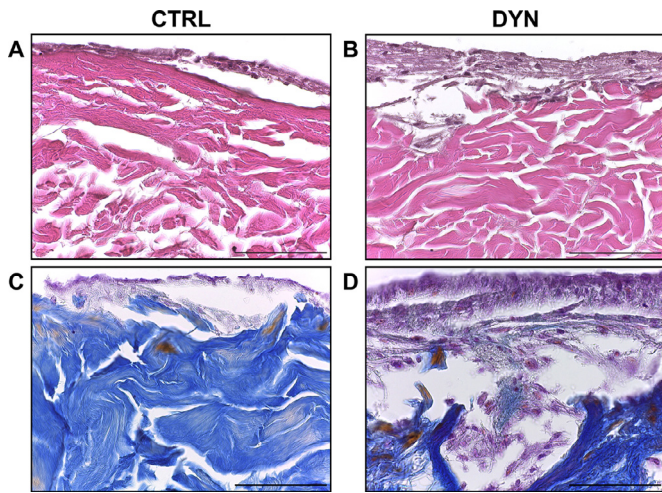


Figure 4. Representative images from histochemical analysis of constructs cultured under static (CTRL) or dynamic (DYN) conditions. Hematoxylin and eosin staining (A, B) and Mallory's trichrome (C, D) staining. Scale bar = 50 μ m.

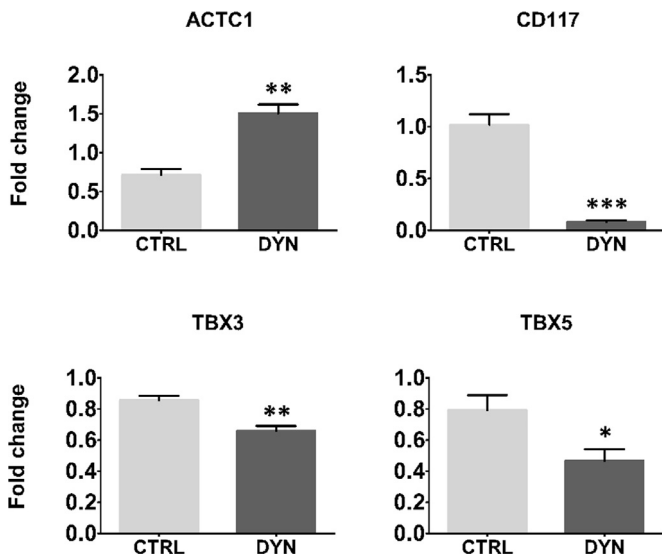


Figure 5. Gene expression analysis for constructs cultured under static (CTRL) or dynamic (DYN) conditions. Expression of ACTC1, typical marker of late differentiating and mature cardiac myocytes, CD117, typical marker of undifferentiated hCPCs, and of TBX-3 and TBX-5, markers of early stages of cardiac myocyte differentiation (* $p \leq 0.05$; ** $p \leq 0.01$; *** $p \leq 0.001$).

ferentiation towards mature cardiac myocytes, in accordance with previous studies [72–76].

Although further and longer experimental tests will be necessary for comprehensively characterizing the effect of cyclic stretch on the maturation of d-HuSk scaffolds seeded with hCPCs, the latter particularly sensitive to the microenvironment, the preliminary promising findings provided evidence of the bioreactor platform reliability and suitability for cardiac tissue engineering applications. In the future, the possibility to switch from stretching to compression mode will be implemented in the bioreactor platform, and the device will be adapted to be equipped with an electrical stimulation unit [77] to provide combinable mechanical and electrical stimulations for mimicking the complex native cardiac environment.

In conclusion, adopting customizable and low-cost technological solutions, a compact, easy-to-use, tunable stretch bioreactor platform for biomimetic dynamic culture of 3D engineered was developed. Based on modular components and providing tunable stim-

ulation, the proposed device is versatile and adaptable for different tissue engineering applications. Moreover, the choice of the 3D printing technology and low-cost hardware coupled with free and open-source software, substantially limited the development costs and will support in the future the use of the system as valuable tool for *in vitro* investigation and for future production of functional engineered constructs.

Declaration of Competing Interest

The authors declare that the research was conducted in the absence of any commercial or financial relationships that could be construed as a potential conflict of interest.

Acknowledgements

None.

Ethical approval

Patients provided written informed consent and samples were collected without patient identifiers, following protocols approved by the Federico II University Hospital Ethical Committee (ref. number 79/18) and in conformity with principles outlined in the Declaration of Helsinki.

Supplementary materials

Supplementary material associated with this article can be found, in the online version, at [doi:10.1016/j.medengphy.2020.07.018](https://doi.org/10.1016/j.medengphy.2020.07.018).

References

- [1] Lanza R, Langer R, Vacanti J. Principles of tissue engineering. 4th editor. Elsevier; 2014. doi:10.1016/C2011-0-07193-4.
- [2] Vunjak Novakovic G, Eschenhagen T, Mummery C. Myocardial tissue engineering: *in vitro* models. Cold Spring Harb Perspect Med 2014;4:a014076. doi:10.1101/cshperspect.a014076.
- [3] Goldstein AS, Christ G. Functional tissue engineering requires bioreactor strategies. Tissue Eng Part A 2009;15:739–40. doi:10.1089/ten.tea.2009.0046.
- [4] Lyons F, Partap S, O'Brien FJ. Part 1: scaffolds and surfaces. Technol Heal Care 2008;16:305–17. doi:10.3233/THC-2008-16409.
- [5] Kropp C, Massai D, Zweigerdt R. Progress and challenges in large-scale expansion of human pluripotent stem cells. Process Biochem 2017;59:244–54. doi:10.1016/j.procbio.2016.09.032.
- [6] Chimenti I, Massai D, Morbiducci U, Beltrami AP, Pesce M, Messina E. Stem cell spheroids and *ex vivo* niche modeling: rationalization and scaling-up. J Cardiovasc Transl Res 2017;10:150–66. doi:10.1007/s12265-017-9741-5.
- [7] Bianco P, Robey PG. Stem cells in tissue engineering. Nature 2001;414:118–21. doi:10.1038/35102181.
- [8] Caplan AI. Adult mesenchymal stem cells for tissue engineering versus regenerative medicine. J Cell Physiol 2007;213:341–7. doi:10.1002/jcp.21200.
- [9] Kwon SG, Kwon YW, Lee TW, Park GT, Kim JH. Recent advances in stem cell therapeutics and tissue engineering strategies. Biomater Res 2018;22:36. doi:10.1186/s40824-018-0148-4.
- [10] Edri R, Gal I, Noor N, Harel T, Fleischer S, Adadi N, et al. Personalized hydrogels for engineering diverse fully autologous tissue implants. Adv Mater 2019;31:1803895. doi:10.1002/adma.201803895.
- [11] Badyal SF, Taylor D, Uygun K. Whole-organ tissue engineering: decellularization and recellularization of three-dimensional matrix scaffolds. Annu Rev Biomed Eng 2011;13:27–53. doi:10.1146/annurev-bioeng-071910-124743.
- [12] Porzionato A, Stocco E, Barbon S, Grandi F, Macchi V, De Caro R. Tissue-engineered grafts from human decellularized extracellular matrices: a systematic review and future perspectives. Int J Mol Sci 2018;19:4117. doi:10.3390/ijms19124117.
- [13] Murphy WL, McDevitt TC, Engler AJ. Materials as stem cell regulators. Nat Mater 2014;13:547–57. doi:10.1038/nmat3937.
- [14] Guilak F, Butler DL, Goldstein SA, Baajens FPT. Biomechanics and mechanobiology in functional tissue engineering. J Biomech 2014;47:1933–40. doi:10.1016/j.jbiomech.2014.04.019.
- [15] Almouemen N, Kelly HM, O'Leary C. Tissue engineering: understanding the role of biomaterials and biophysical forces on cell functionality through computational and structural biotechnology analytical methods. Comput Struct Biotechnol J 2019;17:591–8. doi:10.1016/j.csbj.2019.04.008.

- [16] Vunjak-Novakovic G, Tandon N, Godier A, Maidhof R, Marsano A, Martens TP, et al. Challenges in cardiac tissue engineering. *Tissue Eng Part B Rev* 2010;16:169–87. doi:10.1089/ten.teb.2009.0352.
- [17] Martin I, Wendt D, Heberer M. The role of bioreactors in tissue engineering. *Trends Biotechnol* 2004;22:80–6. doi:10.1016/j.tibtech.2003.12.001.
- [18] Bilodeau K, Mantovani D. Bioreactors for tissue engineering: focus on mechanical constraints. A comparative review. *Tissue Eng* 2006;12:2367–83. doi:10.1089/ten.2006.12.2367.
- [19] Ravichandran A, Liu Y, Teoh S-H. Review: bioreactor design towards generation of relevant engineered tissues: focus on clinical translation. *J Tissue Eng Regen Med* 2018;12:e7–22. doi:10.1002/term.2270.
- [20] Mantero S, Sadr N, Riboldi SA, Lorenzoni S, Montevecchi FM. A new electro-mechanical bioreactor for soft tissue engineering. *J Appl Biomater Biomech* 2007;5:107–16.
- [21] Powell CA, Smiley BL, Mills J, Vandenberg HH. Mechanical stimulation improves tissue-engineered human skeletal muscle. *Am J Physiol Physiol* 2002;283:C1557–65. doi:10.1152/ajpcell.00595.2001.
- [22] Moon DG, Christ G, Stitzel JD, Atala A, Yoo JJ. Cyclic mechanical preconditioning improves engineered muscle contraction. *Tissue Eng Part A* 2008;14:473–82. doi:10.1089/tea.2007.0104.
- [23] Somers SM, Spector AA, DiGirolamo DJ, Grayson WL. Biophysical stimulation for engineering functional skeletal muscle. *Tissue Eng Part B Rev* 2017;23:362–72. doi:10.1089/ten.teb.2016.0444.
- [24] Turner DC, Kasper AM, Seaborne RA, Brown AD, Close GL, Murphy M, et al. Exercising bioengineered skeletal muscle in vitro: biopsy to bioreactor. *Methods Mol Biol*. 2019;1889:55–79. doi:10.1007/978-1-4939-8897-6_5.
- [25] Paxton JZ, Hagerty P, Andrick JJ, Baar K. Optimizing an intermittent stretch paradigm using ERK1/2 phosphorylation results in increased collagen synthesis in engineered ligaments. *Tissue Eng Part A* 2012;18:277–84. doi:10.1089/ten.tea.2011.0336.
- [26] Wang T, Gardiner BS, Lin Z, Rubenson J, Kirk TB, Wang A, et al. Bioreactor design for tendon/ligament engineering. *Tissue Eng Part B Rev* 2013;19:133–46. doi:10.1089/ten.teb.2012.0295.
- [27] Youngstrom DW, Rajpar I, Kaplan DL, Barrett JG. A bioreactor system for in vitro tendon differentiation and tendon tissue engineering. *J Orthop Res* 2015;33:911–18. doi:10.1002/jor.22848.
- [28] Burk J, Plenge A, Brehm W, Heller S, Pfeiffer B, Kasper C. Induction of tenogenic differentiation mediated by extracellular tendon matrix and short-term cyclic stretching. *Stem Cells Int* 2016;2016:1–11. doi:10.1155/2016/7342379.
- [29] Dursun G, Tohidnezhad M, Markert B, Stoffel M. Effects of uniaxial stretching on tenocyte migration behaviour. *Curr Dir Biomed Eng* 2018;4:313–17. doi:10.1515/cdbme-2018-0076.
- [30] Talò D, D'Arrigo D, Lorenzi S, Moretti M, Lovati AB. Independent, controllable stretch-perfusion bioreactor chambers to functionalize cell-seeded decellularized tendons. *Ann Biomed Eng* 2020;48:1112–26. doi:10.1007/s10439-019-02257-6.
- [31] Tokuyama E, Nagai Y, Takahashi K, Kimata Y, Naruse K. Mechanical stretch on human skin equivalents increases the epidermal thickness and develops the basement membrane. *PLoS One* 2015;10:e0141989. doi:10.1371/journal.pone.0141989.
- [32] Jeong C, Chung HY, Lim HJ, Lee JW, Choi KY, Yang JD, et al. Applicability and safety of in vitro skin expansion using a skin bioreactor: a clinical trial. *Arch Plast Surg* 2014;41:661. doi:10.5999/aps.2014.41.6.661.
- [33] Huh M-I, Yi S-J, Lee K-P, Kim HK, An S-H, Kim D-B, et al. Full thickness skin expansion ex vivo in a newly developed reactor and evaluation of auto-grafting efficiency of the expanded skin using yucatan pig model. *Tissue Eng Regen Med* 2018;15:629–38. doi:10.1007/s13770-018-0154-6.
- [34] Zimmermann W-H, Schneiderbanger K, Schubert P, Didié M, Münzel F, Heubach JF, et al. Tissue engineering of a differentiated cardiac muscle construct. *Circ Res* 2002;90:223–30. doi:10.1161/hh0202.103644.
- [35] Zimmermann W-H, Melnychenko I, Wasmeier G, Didié M, Naito H, Nixdorff U, et al. Engineered heart tissue grafts improve systolic and diastolic function in infarcted rat hearts. *Nat Med* 2006;12:452–8. doi:10.1038/nm1394.
- [36] Birla RK, Huang YC, Dennis RG. Development of a novel bioreactor for the mechanical loading of tissue-engineered heart muscle. *Tissue Eng* 2007;13:2239–48. doi:10.1089/ten.2006.0359.
- [37] Schaaf S, Shibamiya A, Mewe M, Eder A, Stöhr A, Hirt MN, et al. Human engineered heart tissue as a versatile tool in basic research and preclinical toxicology. *PLoS One* 2011;6:e26397. doi:10.1371/journal.pone.0026397.
- [38] Mihic A, Li J, Miyagi Y, Gagliardi M, Li S-H, Zu J, et al. The effect of cyclic stretch on maturation and 3D tissue formation of human embryonic stem cell-derived cardiomyocytes. *Biomaterials* 2014;35:2798–808. doi:10.1016/j.biomaterials.2013.12.052.
- [39] Salazar BH, Cashion AT, Dennis RG, Birla RK. Development of a cyclic strain bioreactor for mechanical enhancement and assessment of bioengineered myocardial constructs. *Cardiovasc Eng Technol* 2015;6:533–45. doi:10.1007/s13239-015-0236-8.
- [40] Mannhardt I, Breckwoldt K, Letuffe-Brenière D, Schaaf S, Schulz H, Neuber C, et al. Human engineered heart tissue: analysis of contractile force. *Stem Cell Reports* 2016;7:29–42. doi:10.1016/j.stemcr.2016.04.011.
- [41] Morgan K.Y., Black L.D. Creation of a bioreactor for the application of variable amplitude mechanical stimulation of fibrin gel-based engineered cardiac tissue. 2014, p. 177–87. https://doi.org/10.1007/978-1-4939-1047-2_16.
- [42] Valls-Margarit M, Iglesias-García O, Di Guglielmo C, Sarlabous L, Tadevosyan K, Paoli R, et al. Engineered macroscale cardiac constructs elicit human myocardial tissue-like functionality. *Stem Cell Rep* 2019;13:207–20. doi:10.1016/j.stemcr.2019.05.024.
- [43] Hambor JE. Bioreactor design and bioprocess controls for industrialized cell processing: bioengineering strategies and platform technologies. *Bioprocess Int* 2012;10:22–33.
- [44] Hansmann J, Groeber F, Kahlig A, Kleinhans C, Walles H. Bioreactors in tissue engineering—principles, applications and commercial constraints. *Biotechnol J* 2013;8:298–307. doi:10.1002/biot.201200162.
- [45] Ozturk S, Hu WS. *Cell culture technology for pharmaceutical and cell-based therapies*. CRC Press; 2005.
- [46] Martin I, Smith T, Wendt D. Bioreactor-based roadmap for the translation of tissue engineering strategies into clinical products. *Trends Biotechnol* 2009;27:495–502. doi:10.1016/j.tibtech.2009.06.002.
- [47] Wendt D, Riboldi SA, Cioffi M, Martin I. Potential and bottlenecks of bioreactors in 3D cell culture and tissue manufacturing. *Adv Mater* 2009;21:3352–67. doi:10.1002/adma.200802748.
- [48] Raveling AR, Theodossiou SK, Schiele NR. A 3D printed mechanical bioreactor for investigating mechanobiology and soft tissue mechanics. *MethodsX* 2018;5:924–32. doi:10.1016/j.mex.2018.08.001.
- [49] Schneider D, Tschernich J, Scharin-Mehlmann M, Gilbert DF. 3D-printed reusable cell culture chamber with integrated electrodes for electrical stimulation and parallel microscopic evaluation. *3D Print Addit Manuf* 2018;5:115–25. doi:10.1089/3dp.2017.0103.
- [50] Smith LJ, Li P, Holland MR, Ekser B. FABRICA: a bioreactor platform for printing, perfusing, observing, & stimulating 3D tissues. *Sci Rep* 2018;8:7561. doi:10.1038/s41598-018-25663-7.
- [51] Rimington RP, Capel AJ, Chaplin KF, Fleming JW, Bandulasena HCH, Bibb RJ, et al. Differentiation of bioengineered skeletal muscle within a 3d printed perfusion bioreactor reduces atrophic and inflammatory gene expression. *ACS Biomater Sci Eng* 2019;5:5525–38. doi:10.1021/acsbomaterials.9b00975.
- [52] Tandon N, Taubman A, Cimetta E, Saccenti L, Vunjak-Novakovic G. Portable bioreactor for perfusion and electrical stimulation of engineered cardiac tissue. In: Proceedings of the 35th Annual International Conference of the IEEE Engineering in Medicine and Biology Society. IEEE; 2013. p. 6219–23. doi:10.1109/EMBC.2013.6610974.
- [53] Pisani G, Massai D, Rodriguez A, Cerino G, Galluzzi R, Labate Falvo D'Urso G, et al. An automated adaptive bioreactor – based platform for culturing cardiac tissue models. In: Proceedings of the V Meeting. Italian Chapter of the European Society of Biomechanics; 2015.
- [54] Putame G, Terzini M, Carbonaro D, Pisani G, Serino G, Di Meglio F, et al. Application of 3D printing technology for design and manufacturing of customized components for a mechanical stretching bioreactor. *J Healthc Eng* 2019;2019:1–9. doi:10.1155/2019/3957931.
- [55] Massai D, Pisani G, Isu G, Rodriguez Ruiz A, Cerino G, Galluzzi R, et al. Bioreactor platform for biomimetic culture and in situ monitoring of the mechanical response of in vitro engineered models of cardiac tissue. *Front Bioeng Biotechnol* 2020;8. doi:10.3389/fbioe.2020.00733.
- [56] Carbonaro D, Putame G, Castaldo C, Di Meglio F, Belviso I, Sacco AM, et al. A novel 3D-printed sample-holder for agitation-based decellularization - human cardiac tissue application. In: Proceeding 25th Congress of the European Society of Biomechanics, ESB 2019; 2019. p. 546.
- [57] Di Meglio F, Nurzynska D, Romano V, Miraglia R, Belviso I, Sacco AM, et al. Optimization of human myocardium decellularization method for the construction of implantable patches. *Tissue Eng Part C Methods* 2017;23:525–39. doi:10.1089/ten.tec.2017.0267.
- [58] Belviso I, Romano V, Sacco AM, Ricci G, Massai D, Cammarota M, et al. Decellularized human dermal matrix as a biological scaffold for cardiac repair and regeneration. *Front Bioeng Biotechnol* 2020;8. doi:10.3389/fbioe.2020.00229.
- [59] Nurzynska D, Di Meglio F, Romano V, Miraglia R, Sacco AM, Latino F, et al. Cardiac primitive cells become committed to a cardiac fate in adult human heart with chronic ischemic disease but fail to acquire mature phenotype: genetic and phenotypic study. *Basic Res Cardiol* 2013;108:320. doi:10.1007/s00395-012-0320-2.
- [60] Schneck D. *An outline of cardiovascular structure and function. Biomedical engineering handbook*. Bronzino J, Peterson D, editors. CRC Press; 2018. Four vol. set.
- [61] Klingensmith M., Ern Chen L., Glasgow S., Goers T., Melly S. *The Washington manual of surgery*. 2008.
- [62] Kuznetsova T, Herbots L, Richart T, D'hooge J, Thijs L, Fagard RH, et al. Left ventricular strain and strain rate in a general population. *Eur Heart J* 2008;29:2014–23. doi:10.1093/eurheartj/ehn280.
- [63] Kensah G, Roa Lara A, Dahlmann J, Zweigert R, Schwanke K, Hegemann J, et al. Murine and human pluripotent stem cell-derived cardiac bodies form contractile myocardial tissue in vitro. *Eur Heart J* 2013;34:1134–46. doi:10.1093/eurheartj/ehs349.
- [64] Sacco AM, Belviso I, Romano V, Carfora A, Schonauer F, Nurzynska D, et al. Diversity of dermal fibroblasts as major determinant of variability in cell reprogramming. *J Cell Mol Med* 2019;23:4256–68. doi:10.1111/jcmm.14316.
- [65] Cerino G, Gaudiello E, Grussenmeyer T, Melly L, Massai D, Banfi A, et al. Three dimensional multi-cellular muscle-like tissue engineering in perfusion-based bioreactors. *Biotechnol Bioeng* 2016;113:226–36. doi:10.1002/bit.25688.
- [66] Schmid J, Schwarz S, Meier-Staude R, Sudhop S, Clausen-Schaumann H, Schieker M, et al. A perfusion bioreactor system for cell seeding and oxygen-controlled cultivation of three-dimensional cell cultures. *Tissue Eng Part C Methods* 2018;24:585–95. doi:10.1089/ten.tec.2018.0204.

- [67] Piola M, Prandi F, Bono N, Soncini M, Penza E, Agrifoglio M, et al. A compact and automated ex vivo vessel culture system for the pulsatile pressure conditioning of human saphenous veins. *J Tissue Eng Regen Med* 2016;10:E204–15. doi:[10.1002/term.1798](https://doi.org/10.1002/term.1798).
- [68] Chen CS. Mechanotransduction – a field pulling together? *J Cell Sci* 2008;121:3285–92. doi:[10.1242/jcs.023507](https://doi.org/10.1242/jcs.023507).
- [69] Paluch EK, Nelson CM, Biais N, Fabry B, Moeller J, Pruitt BL, et al. Mechanotransduction: use the force(s). *BMC Biol* 2015;13:47. doi:[10.1186/s12915-015-0150-4](https://doi.org/10.1186/s12915-015-0150-4).
- [70] Humphrey JD, Dufresne ER, Schwartz MA. Mechanotransduction and extracellular matrix homeostasis. *Nat Rev Mol Cell Biol* 2014;15:802–12. doi:[10.1038/nrm3896](https://doi.org/10.1038/nrm3896).
- [71] Martino F, Perestrelo AR, Vinarský V, Pagliari S, Forte G. Cellular mechanotransduction: from tension to function. *Front Physiol* 2018;9:1–21. doi:[10.3389/fphys.2018.00824](https://doi.org/10.3389/fphys.2018.00824).
- [72] Massai D, Cerino G, Gallo D, Pennella F, Deriu M, Rodriguez A, et al. Bioreactors as engineering support to treat cardiac muscle and vascular disease. *J Healthc Eng* 2013;4:329–70. doi:[10.1260/2040-2295.4.3.329](https://doi.org/10.1260/2040-2295.4.3.329).
- [73] Liaw NY, Zimmermann W. Mechanical stimulation in the engineering of heart muscle. *Adv Drug Deliv Rev* 2016;96:156–60. doi:[10.1016/j.addr.2015.09.001](https://doi.org/10.1016/j.addr.2015.09.001).
- [74] Parsa H, Ronaldson K, Vunjak-Novakovic G. Bioengineering methods for myocardial regeneration. *Adv Drug Deliv Rev* 2016;96:195–202. doi:[10.1016/j.addr.2015.06.012](https://doi.org/10.1016/j.addr.2015.06.012).
- [75] Stoppel WL, Kaplan DL, Black LD. Electrical and mechanical stimulation of cardiac cells and tissue constructs. *Adv Drug Deliv Rev* 2016;96:135–55. doi:[10.1016/j.addr.2015.07.009](https://doi.org/10.1016/j.addr.2015.07.009).
- [76] Paez-Mayorga J, Hernández-Vargas G, Ruiz-Esparza GU, Iqbal HMN, Wang X, Zhang YS, et al. Bioreactors for cardiac tissue engineering. *Adv Healthc Mater* 2019;8:1701504. doi:[10.1002/adhm.201701504](https://doi.org/10.1002/adhm.201701504).
- [77] Gabetti S, Putame G, Montrone F, Isu G, Marsano A, Audenino A, et al. Versatile electrical stimulator for providing cardiac-like electrical impulses in vitro. *Biomed Sci Eng* 2020;3. doi:[10.4081/bse.2019.111](https://doi.org/10.4081/bse.2019.111).